THEORETICAL AND APPLIED MECHANICS
Article in Press (2016) DOI: 10.2298/TAM151029001W

# TORSION OF ELLIPTICAL COMPOSITE BARS CONTAINING NEUTRAL COATED CAVITIES

**Xu Wang, Cuiying Wang, and Peter Schiavone**

Abstract. Using complex variable methods and conformal mapping techniques, we establish the existence of coated cavities of various shapes that do not disturb the warping function in a host elliptical bar. These cavities are known as 'partly neutral cavities'. Our results show that the two axes corresponding to the neutral elliptical coating are parallel to those of the host elliptical bar and that the centre of the elliptical coating can be located arbitrarily on the major axis of the host bar. Examples of neutral coated non-elliptical cavities are provided.

## 1. Introduction

The construction of 'neutral inhomogeneities' in the Saint-Venant theory of torsion of composite bars can be achieved through the introduction of a thin interphase of low shear modulus (the LS-type interface) or a thin interphase of high shear modulus (the HS-type interface) as well as through the introduction of a thick coating [**1**, **3**]. A 'neutral inhomogeneity' will not disturb the warping function in a host bar (partial neutrality) and in some cases will additionally not alter the original torsional stiffness (complete neutrality) after its introduction in a homogeneous cylindrical bar. Benveniste and Chen [**1**] discussed the neutrality of a soft elliptical inhomogeneity with a variable HS-type interface embedded in a host bar of elliptical cross section. They derived analytical expressions for the variable interface parameter and discussed the neutrality of a stiff circular inhomogeneity with a constant LS-type interface inserted in a host circular bar. Chen et al. [**3**] demonstrated the existence of thickly coated neutral inhomogeneities of various shapes in a host circular bar. In their discussion of a coated cavity, Chen et al. [**3**] noted that the coating must be stiffer than the host bar. Investigations on neutral inhomogeneities in various contexts other than in the Saint-Venant theory of torsion have been undertaken by various authors in the literature (see, for example, [**2**, **4**–**9**]). In this study, we focus on the partial neutrality of both thickly and thinly coated cavities of various shapes in the Saint-Venant torsion of a compound bar of elliptical cross

2010 *Mathematics Subject Classification:* 74B05; 74E30; 30E25.
*Key words and phrases:* Saint-Venant torsion; elliptical bar; neutral coated cavities; complex variable method; conformal mapping.

section. Using complex variable methods and conformal mapping techniques, we demonstrate the existence of a rich class of coated elliptical or non-elliptical cavities that leave the warping function in the host elliptical bar undisturbed. We show that the coating can be stiffer as well as softer than the host bar in order to achieve neutrality.

## 2. Neutral Coated Cavities

We establish a Cartesian coordinate system $\{x_i\}$ $(i = 1, 2, 3)$ and consider the Saint-Venant torsion problem of an elliptical cylindrical bar with homogeneous shear modulus denoted by $\mu_m$. The boundary of the elliptical bar is described by the equation $x_1^2/a^2 + x_2^2/b^2 = 1$ with $a$ and $b$ being the semi-major and semi-minor axes of the ellipse, respectively. We ask which shape of coated cavity will not disturb the warping function in the elliptical bar when inserted into the host elliptical bar (the matrix). In the following analysis, the subscripts $c$ and $m$ are used to identify the respective quantities in the coating and the matrix.

It is well-known that the displacement field corresponding to Saint-Venant torsion is characterized by

$$u_1 = -\vartheta x_2 x_3, \quad u_2 = \vartheta x_1 x_3, \quad u_3 = \vartheta \varphi(x_1, x_2),$$

where $\vartheta$ is the angle of twist per unit length of the bar and $\varphi$ is the warping function. The equilibrium condition $\sigma_{ij,j} = 0$ ($j = 1, 2, 3$ and we sum over repeated indices) requires that $\varphi$ is harmonic throughout the cross-section of the cylinder. The two shear stress components are given by

$$\sigma_{31} = \vartheta\mu(\varphi_{,1} - x_2), \quad \sigma_{32} = \vartheta\mu(\varphi_{,2} + x_1),$$

where $\mu$ is the shear modulus.

Since $\varphi$ is harmonic, we can construct the analytic function $f(z) = \psi + \mathrm{i}\,\varphi$ of the complex variable $z = x_1 + \mathrm{i}\,x_2$ where $\psi$ is the conjugate harmonic function. Consequently, the shear stresses can be concisely expressed in terms of $f(z)$ as follows

$$\sigma_{32} + \mathrm{i}\,\sigma_{31} = \vartheta\mu[f'(z) + \bar{z}],$$

It is assumed that the coating and the surrounding matrix are perfectly bonded at the interface $\Gamma$. The continuity conditions of displacement and traction across the interface $\Gamma$ can be expressed as

$$\varphi_c - \varphi_m = 0, \quad \mu_c\psi_c - \mu_m\psi_m = \frac{1}{2}(\mu_m - \mu_c)z\bar{z} + \text{const}, \quad z \in \Gamma \tag{2.1}$$

The traction-free condition on the inner surface $L$ of the coating is given by

$$\vartheta_c = -\frac{1}{2}z\bar{z} + \text{const}, \quad z \in L. \tag{2.2}$$

Equation (2.1) can be equivalently expressed in terms of the two analytic functions $f_c(z)$ defined in the coating and $f_m(z)$ defined in the matrix as follows

$$\begin{aligned} &f_c(z) - \overline{f_c(z)} = f_m(z) - \overline{f_m(z)}, \\ &f_c(z) + \overline{f_c(z)} = \lambda\Big[f_m(z) + \overline{f_m(z)}\Big] + (\lambda - 1)z\bar{z} + \text{const}, \quad z \in \Gamma, \end{aligned} \tag{2.3}$$

where $\lambda = \mu_m/\mu_c$. Similarly, condition (2.2) can be expressed in terms of $f_c(z)$ as

$$f_c(z) + \overline{f_c(z)} = -z\bar{z} + \text{const}, \quad z \in L. \tag{2.4}$$

Adding the two conditions in Eq. (2.3) together, we obtain

$$f_c(z) = \frac{\lambda+1}{2}\overline{f_m(z)} + \frac{\lambda-1}{2}z\bar{z} + \text{const}, \quad z \in \Gamma. \tag{2.5}$$

Since the analytic function $f_m(z)$ in the host bar is not disturbed by the coated cavity, we have [**10**]

$$f_m(z) = -\frac{m}{1+m^2}z^2, \tag{2.6}$$

where $m = (a-b)/(a+b)$. When the host bar has a circular cross section ($a = b$), we obtain from Eq. (2.6) that $f_m(z) \equiv 0$. This is simply the case of a vanishing warping function discussed by Chen et al. [**3**].

Substitution of Eq. (2.6) into Eq. (2.5) leads to

$$f_c(z) = \frac{\lambda-1}{2}z\bar{z} - \frac{m(\lambda+1)}{2(1+m^2)}z^2 + \frac{m(1-\lambda)}{2(1+m^2)}\bar{z}^2 + \text{const}, \quad z \in \Gamma. \tag{2.7}$$

We now introduce the following conformal mapping function

$$z = \omega(\xi) = \sum_{n=-\infty}^{\infty} a_n \xi^n, \quad r \leqslant |\xi| \leqslant 1, \tag{2.8}$$

which maps the coating in the $z$-plane onto an annulus with inner radius $r$ and outer unit radius in the $\xi$-plane. In particular, the coating-matrix interface $\Gamma$ is mapped onto $|\xi| = 1$ and the inner surface $L$ of the coating is mapped to $|\xi| = r$. In order to ensure that the mapping is one-to-one (or conformal), we must have $\omega'(\xi) \neq 0$ for $r \leqslant |\xi| \leqslant 1$. Our task below is to determine the complex coefficients $a_n$ so that the coating will not disturb the warping function in the host bar.

The analytic function $f_c(\xi) = f_c(\omega(\xi))$ can be expanded in the following Laurent series

$$f_c(\xi) = \sum_{n=-\infty}^{\infty} b_n \xi^n, \quad r \leqslant |\xi| \leqslant 1, \tag{2.9}$$

where $b_n$ are unknown complex coefficients.

Inserting Eq. (2.9) into Eqs. (2.4) and (2.7) and equating like powers of $\xi$, we arrive at the following relationships

$$\begin{aligned} b_k = {} & \frac{\lambda-1}{2}\sum_{n=-\infty}^{\infty} a_n \bar{a}_{n-k} - \frac{m(\lambda+1)}{2(1+m^2)}\sum_{n=-\infty}^{\infty} a_n a_{k-n} \\ & + \frac{m(1-\lambda)}{2(1+m^2)}\sum_{n=-\infty}^{\infty} \bar{a}_n \bar{a}_{-k-n}, \quad k \neq 0, \end{aligned} \tag{2.10}$$

$$b_k + r^{-2k}\bar{b}_{-k} = -\sum_{n=-\infty}^{\infty} r^{2(n-k)} a_n \bar{a}_{n-k}, \quad \text{for } k \neq 0. \tag{2.11}$$

The compatibility condition between Eqs. (2.10) and (2.11) leads to the following constraints

$$\begin{aligned}(2.12)\quad &\frac{1-\lambda}{2}(r^k+r^{-k})\sum_{n=-\infty}^{\infty}a_{n+k}\bar{a}_n+\frac{m[r^{-k}(\lambda-1)+r^k(\lambda+1)]}{2(1+m^2)}\sum_{n=-\infty}^{\infty}a_n a_{k-n}\\ &+\frac{m[r^k(\lambda-1)+r^{-k}(\lambda+1)]}{2(1+m^2)}\sum_{n=-\infty}^{\infty}\bar{a}_n\bar{a}_{-n-k}\\ &=\sum_{n=-\infty}^{\infty}r^{2n+k}a_{n+k}\bar{a}_n,\quad k=1,2,\ldots,+\infty.\end{aligned}$$

Eq. (2.12) are restrictions on $\lambda, r$ and $a_k$ which ensure that the warping function in the host elliptical bar remains undisturbed after the introduction of the coated cavity. When $m=0$ for a host circular bar, Eq. (2.12) simply reduces to [**3**, Eq. (2.16)].

The solution of the set of nonlinear algebraic equations for the coefficients $\lambda, r$ and $a_k$ is, in general, nontrivial. In the next section, we focus on a particular class of mapping function to illustrate the theory.

## 3. Illustrative Examples

In this section we concentrate on the case in which $a_{\pm n}=0$ for $n=h+1, h+2,\ldots,+\infty$ in the mapping function (2.8). From Eq. (2.12), the $2h+3$ parameters $(a_{-h},\ldots,a_h,\lambda,r)$ should satisfy the following $2h$ equations

$$\begin{aligned}(3.1a)\quad &\Big[\frac{1-\lambda}{2}(r^{2h}+r^{-2h})-1\Big]a_h\bar{a}_{-h}+\frac{m\big[r^{-2h}(\lambda-1)+r^{2h}(\lambda+1)\big]}{2(1+m^2)}a_h^2\\ &+\frac{m\big[r^{2h}(\lambda-1)+r^{-2h}(\lambda+1)\big]}{2(1+m^2)}\bar{a}_{-h}^2=0,\end{aligned}$$

$$\begin{aligned}(3.1b)\quad &\frac{1-\lambda}{2}(r^{2h-1}+r^{-2h+1})(a_{h-1}\bar{a}_{-h}+a_h\bar{a}_{-h+1})\\ &+\frac{m\big[r^{-2h+1}(\lambda-1)+r^{2h-1}(\lambda+1)\big]}{1+m^2}a_{h-1}a_h\\ &+\frac{m\big[r^{2h-1}(\lambda-1)+r^{-2h+1}(\lambda+1)\big]}{1+m^2}\bar{a}_{-h+1}\bar{a}_{-h}\\ &=r^{-1}a_{h-1}\bar{a}_{-h}+ra_h\bar{a}_{-h+1},\end{aligned}$$

$$\begin{aligned}(3.1c)\quad &\frac{1-\lambda}{2}(r^{2h-2}+r^{-2h+2})(a_{h-2}\bar{a}_{-h}+a_{h-1}\bar{a}_{-h+1}+a_h\bar{a}_{-h+2})\\ &+\frac{m\big[r^{-2h+2}(\lambda-1)+r^{2h-2}(\lambda+1)\big]}{2(1+m^2)}(a_{h-1}a_{h-1}+2a_{h-2}a_h)\\ &+\frac{m\big[r^{2h-2}(\lambda-1)+r^{-2h+2}(\lambda+1)\big]}{2(1+m^2)}(\bar{a}_{-h+1}\bar{a}_{-h+1}+2\bar{a}_{-h+2}\bar{a}_{-h})\\ &=(r^{-2}a_{h-2}\bar{a}_{-h}+a_{h-1}\bar{a}_{-h+1}+r^2a_h\bar{a}_{-h+2}),\end{aligned}$$

$$\vdots$$

$$\begin{aligned}(3.1d)\quad &\frac{1-\lambda}{2}(r^2+r^{-2})(a_{-h+2}\bar{a}_{-h}+a_{-h+3}\bar{a}_{-h+1}+\cdots+a_{h-1}\bar{a}_{h-3}+a_h\bar{a}_{h-2})\\ &+\frac{m\big[r^{-2}(\lambda-1)+r^2(\lambda+1)\big]}{2(1+m^2)}(a_ha_{-h+2}+a_{h-1}a_{-h-3}+\ldots\\ &+a_{-h+3}a_{h-1}+a_{-h+2}a_h)\\ &+\frac{m\big[r^2(\lambda-1)+r^{-2}(\lambda+1)\big]}{2(1+m^2)}(\bar{a}_{h-2}\bar{a}_{-h}+\bar{a}_{h-3}\bar{a}_{-h+1}+\ldots\\ &+\bar{a}_{-h+1}\bar{a}_{-h-3}+\bar{a}_{-h}\bar{a}_{h-2})\\ &=r^{-2h+2}a_{-h+2}\bar{a}_{-h}+r^{-2h+4}a_{-h+3}\bar{a}_{-h+1}+\ldots\\ &+r^{2h-4}a_{h-1}\bar{a}_{h-3}+r^{2h-2}a_h\bar{a}_{h-2},\end{aligned}$$

$$\begin{aligned}(3.1e)\quad &\frac{1-\lambda}{2}(r+r^{-1})(a_{-h+1}\bar{a}_{-h}+a_{-h+2}\bar{a}_{-h+1}+\cdots+a_{h-1}\bar{a}_{h-2}+a_h\bar{a}_{h-1})\\ &+\frac{m[r^{-1}(\lambda-1)+r(\lambda+1)]}{2(1+m^2)}(a_ha_{-h+1}+a_{h-1}a_{-h+2}+\ldots\\ &+a_{-h+2}a_{h-1}+a_{-h+1}a_h)\\ &+\frac{m[r(\lambda-1)+r^{-1}(\lambda+1)]}{2(1+m^2)}(\bar{a}_{h-1}\bar{a}_{-h}+\bar{a}_{h-2}\bar{a}_{-h+1}+\ldots\\ &+\bar{a}_{-h+1}\bar{a}_{h-2}+\bar{a}_{-h}\bar{a}_{h-1})\\ &=r^{-2h+1}a_{-h+1}\bar{a}_{-h}+r^{-2h+3}a_{-h+2}\bar{a}_{-h+1}+\ldots\\ &+r^{2h-3}a_{h-1}\bar{a}_{h-2}+r^{2h-1}a_h\bar{a}_{h-1}.\end{aligned}$$

In the following three subsections, we discuss the three specific cases corresponding to $h = 1$, 2 and 3.

**3.1. A confocally coated elliptical cavity.** We consider a confocally coated elliptical cavity with $h = 1$. We first examine the case in which the elliptical coating is at the centre of the host bar ($a_0 = 0$). In this case, it is deduced from Eq. (3.1a) with $h = 1$ that

$$\eta = \frac{\bar{a}_{-1}}{a_1} = \frac{(1+m^2)[2-(1-\lambda)(r^2+r^{-2})] \pm P_1}{2m[r^2(\lambda-1)+r^{-2}(\lambda+1)]} \tag{3.2}$$

where

$$P_1 = \sqrt{(1-m^2)^2[(1-\lambda)(r^2+r^{-2})-2]^2+8m^2(1-\lambda)(r^2+r^{-2})(r-r^{-1})^2}.$$

In addition, we require that $|\eta| \leqslant r^2$ in order to ensure that the mapping function is conformal. Our numerical results indicate that only the minus sign should be taken in Eq. (3.2) and that $\eta$ is always real. The fact that $\eta$ is real implies that the two axes of the elliptical coating simply coincide with the two axes of the host elliptical bar. The following three facts can also be obtained from Eq. (3.1a) with $h = 1$:

(i) When $\lambda = (r^{-2} - r^2)/(r^2 + r^{-2}) < 1$, we have $\eta \equiv 0$ always and the neutral coating is a concentric circular ring.

(ii) When $\lambda = 1$, it can be rigorously deduced that $\eta = mr^2$. The coating and the host bar have identical shear modulus, and the aspect ratio of the inner surface $L$ of the coating is the same as that of the host elliptical bar.

(iii) As $\lambda \to \infty$, $\eta = m$. The coating is vacuous and the aspect ratio of the interface $\Gamma$ is also the same as that of the host elliptical bar.

We illustrate in Figure 1 $\eta$ as a function of $\lambda$ for different values of $m$ in the case $r = \sqrt{0.6}$. The above three conclusions are clearly reflected in Figure 1. It is also observed from Figure 1 that the coating can indeed be stiffer as well as softer than the surrounding matrix, which is in contrast to the result obtained by Chen et al. [**3**] which indicates a stiff elliptical coating when the host bar has a circular cross section. In fact, when the host bar has a circular cross section ($m = 0$), the shape of the neutral elliptical coating characterized $\eta$ is independent of $\lambda = (r^{-1} - r)^2/(r^{-2} + r^2) \leqslant 1$ [**3**]. When the host bar has an elliptical cross section ($m \neq 0$), our results indicate that the shape of the neutral elliptical coating depends on $\lambda$, $r$ and $m$. In addition, we note that the corresponding result of Chen et al. [**3**] can be recovered from our present result by choosing an extremely small value of $m$ (e.g. $m = 10^{-6}$).

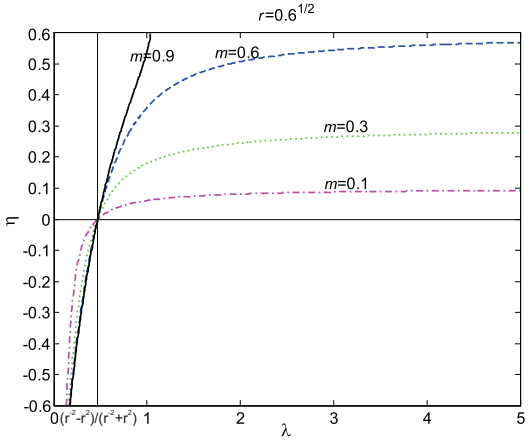


FIGURE 1. Variation of $\eta$ defined in Eq. (3.2) versus $\lambda$ and $m$ with $r = \sqrt{0.6}$.

Next, we consider a non-centred coated elliptical cavity, i.e., $a_0 \neq 0$. In this case condition (3.2) should also be satisfied. In addition, it is deduced from Eq. (3.1b) with $h = 1$ that

$$\chi a_0 - \gamma \bar{a}_0 = 0, \tag{3.3}$$

where

$$\chi = \eta\Big[\frac{1-\lambda}{2}(r + r^{-1}) - r^{-1}\Big] + \frac{m\lfloor r^{-1}(\lambda - 1) + r(\lambda + 1)\rfloor}{1 + m^2},$$

$$\gamma = -\frac{1-\lambda}{2}(r + r^{-1}) + r - \eta\frac{m[r(\lambda-1) + r^{-1}(\lambda+1)]}{1+m^2}.$$

When $|\chi| \neq |\gamma|$, we have from Eq. (3.3) that $a_0 = 0$, which implies that the elliptical coating must be placed at the centre of the host bar. On the other hand, when $|\chi| = |\gamma|$, the coefficient $a_0$ can be chosen arbitrarily. Illustrated in Figure 2 are the calculated pairs $(m, \lambda)$ which satisfy the condition $\chi = \gamma$. In this case, $0 < \lambda < 1$ and $a_0$ is an arbitrary real number. The above fact implies that the coating is stiffer than the matrix and that the centre of the coated elliptical cavity can move arbitrarily along the major axis of the host elliptical bar (the $x_1$-axis) without disturbing the warping function.

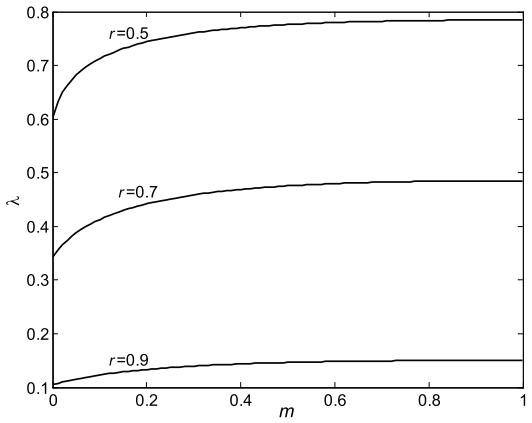


FIGURE 2. The pairs $(m, \lambda)$ which satisfy $\chi = \gamma$.

**3.2. $h = 3$ and $a_{\pm 2} = 0$.** If the mapping function takes the form

$$z = \omega(\xi) = a_3\xi^3 + a_1\xi + a_{-1}\xi^{-1} + a_{-3}\xi^{-3}, \tag{3.4}$$

the following conditions are obtained from Eq. (3.1) with $h = 3$ and $a_{\pm 2} = a_0 = 0$

$$\eta_3 = \frac{\bar{a}_{-3}}{a_3} = \frac{(1+m^2)[2-(1-\lambda)(r^6+r^{-6})] - P_2}{2m[r^6(\lambda-1) + r^{-6}(\lambda+1)]}, \tag{3.5}$$

where

$$P_2 = \sqrt{(1-m^2)^2[(1-\lambda)(r^6+r^{-6}) - 2]^2 + 8m^2(1-\lambda)(r^6+r^{-6})(r^3-r^{-3})^2}$$

$$\eta_1 = \frac{\bar{a}_{-1}}{a_1} = \frac{\frac{1-\lambda}{2}(r^4+r^{-4})\eta_3 - r^{-2}\eta_3 + \frac{m|r^{-4}(\lambda-1)+r^4(\lambda+1)|}{1+m^2}}{r^2 - \frac{1-\lambda}{2}(r^4+r^{-4}) - \frac{m[r^4(\lambda-1)+r^{-4}(\lambda+1)]}{1+m^2}\eta_3} \tag{3.6}$$

$$\frac{a_3}{a_1}\,\mathrm{e}^{-2i\theta} = \frac{2\eta_1 - (1-\lambda)(r^2+r^{-2})\eta_1 - P_3}{(1-\lambda)(r^2+r^{-2})(1+\eta_1\eta_3) - 2(r^4+r^{-4}\eta_1\eta_3) + P_4} \tag{3.7}$$

where $\theta = \arg a_1$,

$$P_3 = \frac{m\{r^{-2}(\lambda-1) + r^2(\lambda+1) + \eta_1^2[r^2(\lambda-1) + r^{-2}(\lambda+1)]\}}{1+m^2},$$

$$P_4 = \frac{2m\{\eta_1[r^{-2}(\lambda-1)+r^2(\lambda+1)]+\eta_3[r^2(\lambda-1)+r^{-2}(\lambda+1)]\}}{1+m^2}.$$

Without loss of generality, we can select $a_1 = 1$. Consequently, for given values of $m$, $r$ and $\lambda$, the parameter $a_3$ can be obtained from Eq. (3.7) while the remaining two parameters $a_{-3}$ and $a_{-3}$ can be obtained from Eqs. (3.5) and (3.6), respectively.

REMARK 3.1. It is seen from Eqs. (3.5)–(3.7) that if we choose $a_1 = \exp(\mathrm{i}\,\theta)$, the resulting shape of the coating is identical to that obtained by choosing $a_1 = 1$.

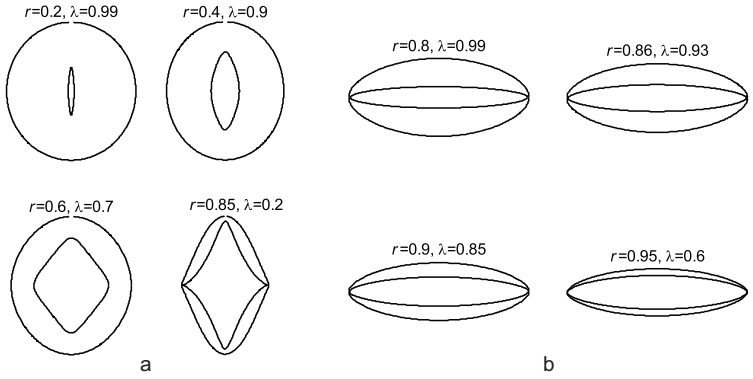


FIGURE 3. Neutral coated cavities in a host elliptical bar with $m = 0.8$ and $\lambda < 1$ described by Eq. (3.4).

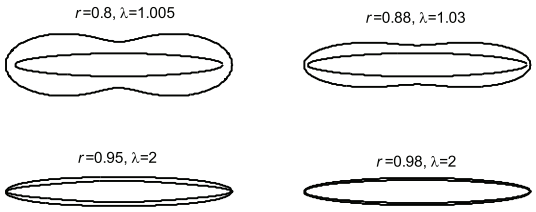


FIGURE 4. Neutral coated cavities in a host elliptical bar with $m = 0.8$ and $\lambda > 1$ described by Eq. (3.4).

The allowable shapes of coated cavities are shown in Figures 3 and 4 with $m = 0.8$ and the resulting parameters $a_3$, $a_{-3}$ and $a_{-3}$ are listed in Table 1. As is seen from Figures 3 and 4, the geometry has a two-fold symmetry. It is also observed from Figures 3 and 4 that the coating can be stiffer as well as softer than the matrix. This result is quite different from that for the case of a host circular bar [**3**]. Chen et al. [**3**] observed that the non-elliptical coating must be stiffer than the host circular bar. The parameter $r$ can be used to characterize the thickness of the coating, and it is seen from Figure 3 that the stiff coating can be very thick ($r \ll 1$) or extremely thin ($r \to 1$). However, it is observed from Figure 4 that the

soft coating is allowed only to be relatively thin (our detailed results indicate that $r > 0.75$). In order to ensure that the mapping is one-to-one, the two parameters $r$ and $\lambda$ cannot be chosen arbitrarily. As illustrated in Figure 5, the pair $(r, \lambda)$ should lie in the two disjointed permissible regions for $\lambda < 1$. In fact the chosen pairs $(r, \lambda)$ in Figure 3(a) lie in the central permissible region in Figure 5 (see the four squares), and the chosen pairs $(r, \lambda)$ in Figure 3(b) lie in the right permissible region in Figure 5 (see the four circles). It is also observed from Figure 6 that the parameter $\lambda(> 1)$ can be chosen arbitrarily when $r > 0.93855$. The four circles in Figure 6 correspond to the chosen pairs $(r, \lambda)$ in Figure 4.

TABLE 1. The three parameters $a_3$, $a_{-1}$ and $a_{-3}$ with $m = 0.8$ and $a_1 = 1$

| | $a_3$ | $a_{-1}$ | $a_{-3}$ |
|---|---|---|---|
| $r = 0.2, \quad \lambda = 0.99$ | $-3.3371 \times 10^{-4}$ | $-0.0320$ | $2.5414 \times 10^{-5}$ |
| $r = 0.4, \quad \lambda = 0.9$ | $-0.0036$ | $-0.0778$ | $0.0010$ |
| $r = 0.6, \quad \lambda = 0.7$ | $-0.0255$ | $-0.0448$ | $0.0143$ |
| $r = 0.85, \ \lambda = 0.2$ | $-0.1493$ | $-0.1056$ | $0.1384$ |
| $r = 0.8, \quad \lambda = 0.99$ | $-0.1418$ | $0.5287$ | $-0.0263$ |
| $r = 0.86, \ \lambda = 0.93$ | $-0.1707$ | $0.5999$ | $-0.0405$ |
| $r = 0.9, \quad \lambda = 0.85$ | $-0.1483$ | $0.6417$ | $-0.0445$ |
| $r = 0.95, \ \lambda = 0.6$ | $-0.1273$ | $0.6857$ | $-0.0482$ |
| $r = 0.8, \quad \lambda = 1.005$ | $0.2060$ | $0.4868$ | $0.0464$ |
| $r = 0.88, \ \lambda = 1.03$ | $0.1543$ | $0.5955$ | $0.0627$ |
| $r = 0.95, \ \lambda = 0.2$ | $0.1091$ | $0.7307$ | $0.0799$ |
| $r = 0.98, \ \lambda = 2$ | $0.0093$ | $0.7815$ | $0.0071$ |

If the mapping function is represented by the following five-term expression

$$z = \omega(\xi) = a_3\xi^3 + a_1\xi + a_0 + a_{-1}\xi^{-1} + a_{-3}\xi^{-3}, \tag{3.8}$$

the following two constraints should also be simultaneously imposed in addition to Eqs. (3.5)–(3.7)

$$\chi_1 a_0 - \gamma \bar{a}_0 = 0, \qquad \chi_3 a_0 - \gamma_3 \bar{a}_0 = 0.$$

Here

$$\chi_1 = \eta_1 \Big[ \frac{1-\lambda}{2}(r + r^{-1}) - r^{-1} \Big] + \frac{m[r^{-1}(\lambda - 1) + r(\lambda + 1)]}{1 + m^2},$$
$$\gamma_1 = -\frac{1-\lambda}{2}(r + r^{-1}) + r - \eta_1 \frac{m[r(\lambda - 1) + r^{-1}(\lambda + 1)]}{1 + m^2},$$
$$\chi_3 = \eta_3 \Big[ \frac{1-\lambda}{2}(r^3 + r^{-3}) - r^{-3} \Big] + \frac{m[r^{-3}(\lambda - 1) + r^3(\lambda + 1)]}{1 + m^2},$$
$$\gamma_3 = -\frac{1-\lambda}{2}(r^3 + r^{-3}) + r^3 - \eta_3 \frac{m[r^3(\lambda - 1) + r^{-3}(\lambda + 1)]}{1 + m^2}$$

We illustrate in Figure 7 the calculated triples $(m, r, \lambda)$ which simultaneously satisfy $\chi_1 = \gamma_1$ and $\chi_3 = \gamma_3$. It has been verified that the mappings obtained by using these triples are indeed one-to-one. In this case, $a_0$ can be an arbitrary real number. This fact implies that the centre of the coated non-elliptical cavity can move arbitrarily along the major axis of the host elliptical bar (the $x_1$-axis) without disturbing the warping function. The case $\lambda < 1$ in Figure 7 indicates that the coating is stiffer than the matrix. The shapes of the non-centred neutral non-elliptical coatings are shown in Figure 8.

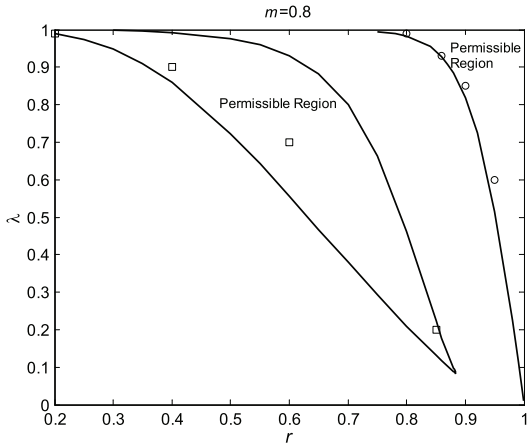


FIGURE 5. The two permissible regions of $r, \lambda$ with $m = 0.8$ and $\lambda < 1$ satisfying a conformal mapping.

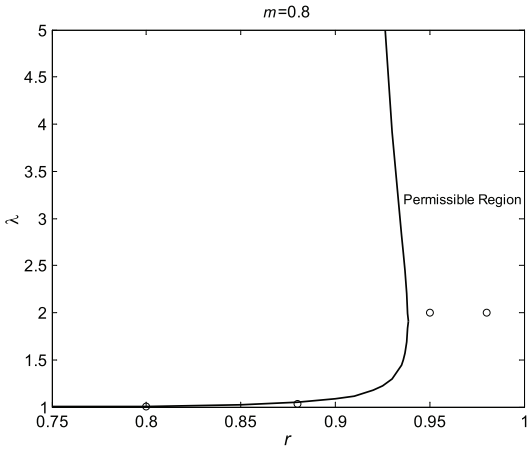


FIGURE 6. The permissible region of $r, \lambda$ with $m = 0.8$ and $\lambda > 1$ satisfying a conformal mapping.

**3.3. $h = 2$.** If we assume that the mapping function takes the following alternative five-term form

$$z = \omega(\xi) = a_2\xi^2 + a_1\xi + a_0 + a_{-1}\xi^{-1} + a_{-2}\xi^{-2}, \tag{3.9}$$

and the coefficients in Eq. (3.9) are assumed to be real, the following conditions can be obtained from Eq. (3.1) with $h = 2$

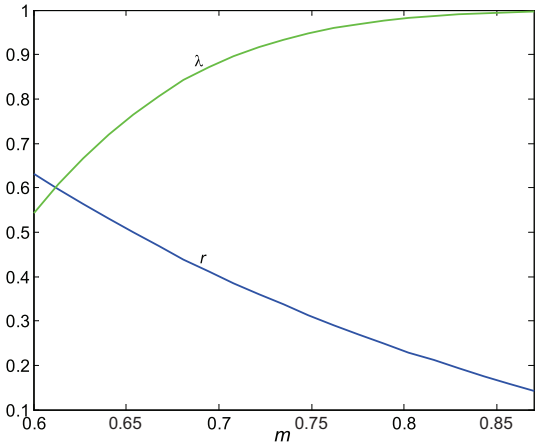


FIGURE 7. The calculated triples $(m, r, \lambda)$ which simultaneously satisfy $\chi_1 = \gamma_1$ and $\chi_3 = \gamma_3$.

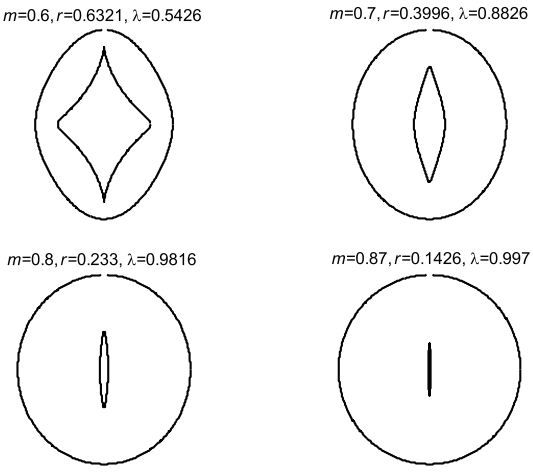


FIGURE 8. Neutral non-centred coated non-elliptical cavities described by Eq. (3.8).

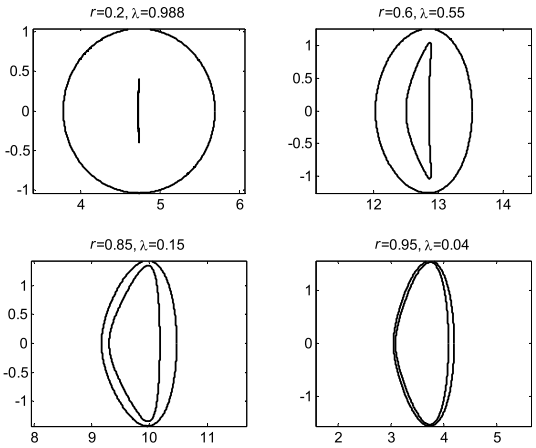


FIGURE 9. Neutral coated cavities described by Eq. (3.9) with $m = 0.8$ and $a_1 = 1$.

$$\eta_2 = \frac{a_{-2}}{a_2} = \frac{(1+m^2)[2-(1-\lambda)(r^4+r^{-4})] \pm P_5}{2m[r^4(\lambda-1)+r^{-4}(\lambda+1)]}, \tag{3.10}$$

where

$$P_5 = \sqrt{(1-m^2)^2[(1-\lambda)(r^4+r^{-4})-2]^2 + 8m^2(1-\lambda)(r^4+r^{-4})(r^2-r^{-2})^2},$$

$$\eta_1 = \frac{a_{-1}}{a_1} = \frac{\frac{1-\lambda}{2}(r^3+r^{-3})\eta_2 - r^{-1}\eta_2 + \frac{m\lfloor r^{-3}(\lambda-1)+r^3(\lambda+1)\rfloor}{1+m^2}}{r - \frac{1-\lambda}{2}(r^3+r^{-3}) - \frac{m[r^3(\lambda-1)+r^{-3}(\lambda+1)]}{1+m^2}\eta_2}, \tag{3.11}$$

$$\frac{a_0 a_2}{a_1^2} = \frac{2\eta_1 - \eta_1(1-\lambda)(r^2+r^{-2}) - P_6}{(1-\lambda)(1+\eta_2)(r^2+r^{-2}) - 2(r^2+\eta_2 r^{-2}) + P_7} \tag{3.12}$$

where

$$P_6 = \frac{m\{r^{-2}(\lambda-1)+r^2(\lambda+1)+\eta_1^2\lfloor r^2(\lambda-1)+r^{-2}(\lambda+1)\rfloor\}}{1+m^2}$$

$$P_7 = \frac{2m\{r^{-2}(\lambda-1)+r^2(\lambda+1)+\eta_2[r^2(\lambda-1)+r^{-2}(\lambda+1)]\}}{1+m^2}$$

$$\frac{a_2}{a_0} = \frac{2(r+\eta_1 r^{-1}) - (1-\lambda)(r+r^{-1})(1+\eta_1) - P_8}{(1-\lambda)(r+r^{-1})(1+\eta_1\eta_2) - 2(r^3+\eta_1\eta_2 r^{-3}) + P_9}, \tag{3.13}$$

where

$$P_8 = \frac{2m\{r^{-1}(\lambda-1)+r(\lambda+1)+\eta_1\lfloor r(\lambda-1)+r^{-1}(\lambda+1\rfloor\}}{1+m^2}$$

$$P_9 = \frac{2m\{\eta_1[r^{-1}(\lambda-1)+r(\lambda+1)]+\eta_2[r(\lambda-1)+r^{-1}(\lambda+1)]\}}{1+m^2}$$

It follows from Eqs. (3.12) and (3.13) that

$$\left(\frac{a_2}{a_1}\right)^2 = \frac{\big(2\eta_1 - \eta_1(1-\lambda)(r^2+r^{-2}) - P_{10}\big)\times P_{11}}{\big((1-\lambda)(r^2+r^{-2})(1+\eta_2) - 2(r^2+\eta_2 r^{-2}) + P_{12}\big)\times P_{13}} \tag{3.14}$$

where

$$\begin{aligned}
P_{10} &= \frac{m\{r^{-2}(\lambda-1)+r^2(\lambda+1)+\eta_1^2[r^2(\lambda-1)+r^{-2}(\lambda+1)]\}}{1+m^2}\\
P_{11} &= 2(r+\eta_1 r^{-1}) - (1-\lambda)(r+r^{-1})(1+\eta_1)\\
&\quad - \frac{2m\{r^{-1}(\lambda-1)+r(\lambda+1)+\eta_1[r(\lambda-1)+r^{-1}(\lambda+1)]\}}{1+m^2}\\
P_{12} &= \frac{2m\{r^{-2}(\lambda-1)+r^2(\lambda+1)+\eta_2[r^2(\lambda-1)+r^{-2}(\lambda+1)]\}}{1+m^2}\\
P_{13} &= (1-\lambda)(r+r^{-1})(1+\eta_1\eta_2) - 2(r^3+\eta_1\eta_2 r^{-3})\\
&\quad + \frac{2m\{\eta_1[r^{-1}(\lambda-1)+r(\lambda+1)]+\eta_2[r(\lambda-1)+r^{-1}(\lambda+1)]\}}{1+m^2}
\end{aligned}$$

We can set $a_1 = 1$, and the remaining coefficients $a_2, a_{-2}, a_{-1}, a_0$ can be obtained from Eqs. (3.10), (3.11), (3.13) and (3.14) for assigned values of $m$, $r$ and $\lambda$. In contrast to the discussions in Subsections 3.1 and 3.2, $a_0$ cannot be arbitrary. We show in Figure 9 the neutral coated cavities described by Eq. (3.9) with $m = 0.8$ and $a_1 = 1$. The geometry in Figure 9 has a one-fold symmetry, and the coating must be stiffer than the surrounding matrix.

## 4. Conclusions

We have successfully designed partly neutral coated cavities for the Saint-Venant torsion of composite cylindrical bars of elliptical cross section. Our analysis is based on complex function theory and conformal mapping. The mapping function (2.8) introduced here maps the coating in the physical $z$-plane onto a circular annulus in the $\xi$-plane. Through satisfaction of the continuity conditions across the coating-matrix interface and the traction-free condition along the inner boundary of the coating, a set of non-linear algebraic equations for the coefficients is obtained. We demonstrate partial neutrality of a confocally coated elliptical cavity and coated non-elliptical cavities using a four-term mapping function in Eq. (3.4) and five-term mapping functions in Eqs. (3.8) and (3.9). It is of particular interest to apply the results found here for neutral coated cavities to the study of the Saint-Venant torsion of a bar of elliptical cross section, in which the bar is filled with neutral coated cavities of the same shape but of varying size.

**Acknowledgments.** This work is supported by the National Natural Science Foundation of China (Grant No: 11272121) and through a Discovery Grant from the Natural Sciences and Engineering Research Council of Canada (Grant #RGPIN 155112).

## References


1. Y. Benveniste, T. Chen, *On the Saint-Venant torsion of composite bars with imperfect interfaces*, Proc. R. Soc. Lond., Ser. A, Math. Phys. Eng. Sci. **457**(2005) (2001), 231–255.
2. Y. Benveniste, T. Miloh, *Neutral inhomogeneities in conduction phenomena*, J. Mech. Phys. Solids **47** (1999), 1873–1892.
3. T. Chen, Y. Benveniste, P. C. Chuang, *Exact solution in torsion of composite bars: thickly coated neutral inhomogeneities and composite cylinder assemblages*, Proc. R. Soc. Lond., Ser. A, Math. Phys. Eng. Sci. **457**(2023) (2002), 1719–1959.
4. Z. Hashin, *The elastic moduli of heterogeneous materials*, J. Appl. Mech. **29** (1962), 143–150.
5. E. H. Mansfield, *Neutral holes in plane sheet-reinforced holes which are equivalent to the uncut sheet*, Q. J. Mech. Appl. Math. **6** (1953), 371–378.
6. G. W. Milton, S. K. Serkov, *Neutral inclusions for conductivity and anti-plane elasticity*, Proc. R. Soc. Lond., Ser. A, Math. Phys. Eng. Sci. **457**(2012) (2001), 1973–1997.
7. C. Q. Ru, *Interface design of neutral elastic inclusions*, Int. J. Solids Struct. **35** (1998), 557–572.
8. X. Wang, P. Schiavone, *Neutral coated circular inclusions in finite plane elasticity of harmonic materials*, Eur. J. Mech., A, Solids **33** (2012), 75–81.
9. X. Wang, P. Schiavone, *Neutrality in the case of N-phase elliptical inclusions with internal uniform hydrostatic stresses*, Int. J. Solids Struct. **49** (2012), 800–807.
10. X. Wang, P. Schiavone, *Torsion of an arbitrarily shaped nanosized bar*, Arch. Appl. Mech. (2015) (In press) DOI: 10.1007/s00419-015-1077-5.

## ТОРЗИЈА ЕЛИПТИЧКИХ КОМПОЗИТНИХ ПОЛУГА КОЈЕ САДРЖЕ НЕУТРАЛНЕ ОБЛОЖЕНЕ ШУПЉИНЕ

Резиме. Користећи метод комплексних променљивих и технику конформалних пресликавања, утврђујемо постојање обложених шупљина различитих облика које не ремете функцију савијања у елиптичној полузи. Ове шупљине су познате као "делимично неутралне шупљине". Наши резултати показују да су две осе које одговарају неутралном елиптичном омотачу паралелне осама елиптичне полуге и да центар елиптичне облоге може бити лоциран произвољно на главној оси полуге. Дати су и примери неутралних обложених не-елиптичних шупљина.

School of Mechanical and Power Engineering
East China University of Science and Technology
Shanghai
China
xuwang@ecust.edu.cn

School of Mechanical and Power Engineering
East China University of Science and Technology
Shanghai
China
cuiyingwang@126.com

Department of Mechanical Engineering
University of Alberta
Alberta
Canada

(Received 29.10.2015.)
(Revised 17.11.2015.)
(Available online 04.03.2016.)